Scheme III

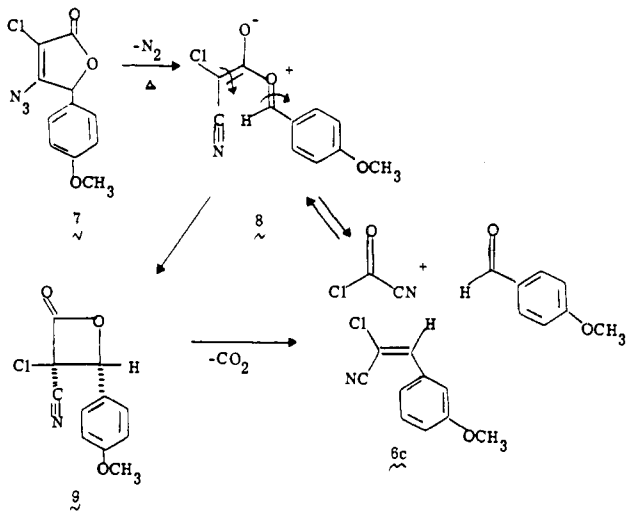

increase as the electron density of the aldehyde carbonyl increases. The opposite trend in product yields was reported by Krabbenhoft[4e] in his analogous study with dichloroketene. (3) The relative rates of the chlorocyanoketene cycloadditions parallel the product yields. For example, generation of chlorocyanoketene in the presence of 1 equiv each of 2,4-dimethoxy- and 4-methoxybenzaldehyde gave a **6a**:**6c** product ratio of 20:1 after 35% conversion, thus indicating that the ketene reacts at least 20 times faster with the more electron-rich aldehyde.

An interesting set of experiments which unambiguously establishes zwitterion **1** as an intermediate in these cycloadditions was accomplished; specifically, the zwitterion was independently generated and its products favorably compared with those obtained in the cycloaddition itself. Based upon our previously reported work on the *zwittazido cleavage* reaction,[7] one would anticipate the thermolysis of 4-azido-3-chloro-5-(4-methoxyphenyl)-2(5*H*)-furanone (**7**)[8] to give zwitterion **8** (Scheme III), the same as that proposed in the cycloaddition of chlorocyanoketene to 4-methoxybenzaldehyde. Indeed, when **7** was subjected to thermolysis in refluxing benzene, an 80% yield of **6c** was realized. Even though a number of mechanisms can be envisaged for the conversion of **7** into **6c**, the zwitterionic mechanism is the most reasonable. Central to such a claim are the following experimental observations. When the furanone **7** was decomposed, as described above, except that 1 equiv of 2,4-dimethoxybenzaldehyde was added, a ratio of 7:1 for **6a**:**6c** was realized after 35% conversion. The fact that both **6a** and **6c** are formed rules out a concerted ring contraction for **7**. A pure ketene mechanism, i.e., one in which **7** exclusively fragments to chlorocyanoketene and 4-methoxybenzaldehyde and these fragments then cycloadd, can also be rejected. That is, if such a mechanism were operative, the **6a**:**6c** ratio should be much greater than the observed 7:1. For example, as shown earlier, the relative rate of cycloaddition of chlorocyanoketene to 2,4-dimethoxybenzaldehyde compared with that of the 4-methoxy analogue is at least 20:1. During the time period for the 35% decomposition of **7** in the above competition experiment, the concentration of the externally added and more reactive 2,4-dimethoxybenzaldehyde would be much greater than that of the internally generated 4-methoxybenzaldehyde. This, coupled with the above-mentioned relative rate differences, would dictate the ratio of **6a**:**6c** to be even greater than 20:1 during this early phase of the reaction. The fact that the observed ratio was 7:1 suggests the most logical interpretation of these data; the azidobutenolide **7** cleaves to the zwitterion **8** and this then partitions between conrotatory ring closure to **9** and equilibration with chlorocyanoketene and 4-methoxybenzaldehyde.

In conclusion, we summarize the significant results to come from this study. (1) Chloro- and bromocyanoketene, unlike other ketenes which have been studied, cycloadd to aryl aldehydes in such a fashion as to impart electrophilic character to the ketene component. (2) The intermediacy of zwitterions such as **1** in the cyanoketene cycloadditions was established, in part, by the previously unprecedented independent generation of one such zwitterion (**8**). (3) From a purely synthetic perspective, these cycloadditions provide a convenient and stereoselective route to (*E*)-1-halo-1-cyano-2-arylethenes.

Acknowledgment. The authors thank the National Science Foundation (CHE-78-02103) and the National Cancer Institute (CA 11890) for financial support of this work.

References and Notes

(1) D. M. Kunert, R. Chambers, F. Mercer, L. Hernandez, Jr., and H. W. Moore, *Tetrahedron Lett.*, 929 (1978).
(2) (a) The mechanism of these cycloadditions has not been unambiguously established, i.e., concerted vs. dipolar. However, in either case the ketene behaves as the nucleophilic component. For representative studies, see W. T. Brady and L. Smith, *J. Org. Chem.*, **36**, 1637 (1971); (b) D. Borrman and R. Wegler, *Chem. Ber.*, **99**, 1245 (1966); (c) D. Borrman and R. Wegler, *ibid.*, **102**, 64 (1969); (d) D. Borrman and R. Wegler, *ibid.*, **100**, 1575 (1967); (e) H. O. Krabbenhoft, *J. Org. Chem.*, **43**, 1305 (1978).
(3) H. W. Moore, L. Hernandez, Jr., and A. Sing, *J. Am. Chem. Soc.*, **98**, 3228 (1976).
(4) ^{13}C NMR and ^{1}H NMR of the crude reaction products show no absorptions corresponding to the *Z* isomers.
(5) W. Adams, J. Baeza, and J. C. Liu, *J. Am. Chem. Soc.*, **94**, 2000 (1972); D. S. Noyes and E. H. Banitt, *J. Org. Chem.*, **31**, 4043 (1966).
(6) The product ratio was determined by ^{1}H NMR analysis of the reaction as a function of time. The percent conversion refers to the percent of disappearance of the ketene precursor at the time the product ratio was measured—approximately 1 h.
(7) H. W. Moore, *Acc. Chem. Res.*, **12**, 125 (1979).
(8) This oil was prepared in 47% yield by treating an ethanolic solution of 3,4-dichloro-5-(4-methoxyphenyl)-2(5*H*)-furanone with NaN_3. The dichloride is a known compound: S. Jung, L. Jung, and P. Cordier, *C.R. Acad. Sci., Ser. C*, **262**, 1793 (1966).

Harold W. Moore,* Frank Mercer
Donna Kunert, Pamela Albaugh
Department of Chemistry, University of California
Irvine, California 92717
Received December 14, 1978

Preparation and Catalytic Properties of Polymer- and Silica-Supported Bimetallic Clusters

Sir:

Bimetallic transition metal clusters hold promise as selective catalysts, offering pairs of neighboring metal centers which, in contrast to those on alloy surfaces, are structurally unique. Supported clusters may be regarded as models of and precursors of bimetallic ("alloy") crystallites on supports, the catalysts used industrially in re-forming of petroleum distillates.[1] We report here preparation of the first supported bimetallic clusters and a demonstration of their catalytic activity.[2] Anchoring of clusters to supports offers the familiar advantages of solid catalysts (ease of separation from reaction products and minimized corrosion) and the prospective advantage of stabilization of coordinatively unsaturated species, which in solution might form aggregated and/or mononuclear species.

We have begun a systematic study of the catalytic behavior of supported bimetallic clusters, using clusters with similar structural units to determine the effects of changes in the metal framework on the catalytic activity. Several bimetallic and monometallic clusters have been attached to phosphine-functionalized poly(styrene–divinylbenzene) and silica by li-

0002-7863/79/1501-5436$01.00/0

Table I. Infrared Spectra of Polymer- and Silica-Supported Clusters and Molecular Analogues[a]

sample	$\nu_{C=O}$, cm^{-1}
$[Fe_2Pt(CO)_8(Ph_2P\text{-}Ⓟ)_2]$	2048 (s), 2002 (s), 1970 (s), 1939 (s)
$[Fe_2Pt(CO)_8(PPh_3)_2]$[b]	2054 (s), 2006 (s), 1984 (sh), 1974 (m), 1956 (m), 1942 (sh), 1878 (w, br)
$[RuPt_2(CO)_5(Ph_2P\text{-}Ⓟ)_3]$	2019 (s), 1949 (s), 1792 (s)
$[RuPt_2(CO)_5(PPh_3)_3]$[b]	2020 (s), 1948 (s), 1845 (w), 1788 (s)
$[HAuOs_3(CO)_{10}(Ph_2P\text{-}Ⓟ)]$	2088 (w), 2067 (w), 2044 (s), 2038 (s, sh), 2012 (m, sh), 2003 (m), 1993 (m), 1976 (m), 1958 (sh), 1939 (w)
$[HAuOs_3(CO)_{10}(Ph_2P\text{-SiL})]$	2088 (w), 2075 (w), 2044 (s, br), 1992 (s, br), 1978 (sh), 1954 (sh)
$[HAuOs_3(CO)_{10}(PPh_3)]$[b]	2091 (m), 2071 (m), 2049 (s), 2041 (s), 2021 (m), 2010 (s), 2002 (s), 1987 (s), 1971 (w, sh)
$[H_4Ru_4(CO)_{12-x}(Ph_2P\text{-SiL})_x]$[c]	2055 (s, sh), 2040 (s, br), 2018 (m), 1998 (s), 1976 (vs, br)
$[H_2Os_3(CO)_9(Ph_2P\text{-SiL})]$[d]	2093 (m), 2067 (w, sh), 2054 (s), 2012 (vs, br), 1972 (sh), 1942 (w)

[a] Absorptions due to the polymer support were subtracted out using a Nicolet 7199 FTIR system. [b] Measured in cyclohexane solution. [c] x = 1, 2, or 3. [d] Also reported by Brown and Evans.[2]

gand exchange. The polymeric support was prepared from the monomers styrene, 2% divinylbenzene, and *p*-bromostyrene, giving 11-μm-thick membranes, which were functionalized with phosphine groups by reaction with $LiPPh_2$.[3] The silica support (Degussa, Aerosil A380) was similarly functionalized by reaction with $PPh_2[CH_2CH_2CH_2Si(OCH_3)_3]$, giving a 0.5% phosphorus content.[4]

Each cluster was prepared by contacting a solution containing a cluster compound with suspended particles of the functionalized support. A swelling solvent, e.g., THF or toluene, had to be used with the polymers. The supported clusters were identified by comparison of their carbonyl infrared spectra with those of the known molecular species.[5]

The preparation in some cases gave supported clusters with unique structures (Table I). In general, the conditions required for the phosphine-substituted clusters to undergo phosphine–polymer ligand exchange were less severe than the conditions required for the nonsubstituted carbonyl clusters to undergo CO–polymer ligand exchange. Most of the cluster attachments were carried out with the phosphine-substituted cluster as the precursor.

Reaction of $[Fe_2Pt(CO)_9(PPh_3)]$[6] with the functionalized poly(styrene–divinylbenzene) in THF for 12 h at 25 °C yielded $[Fe_2Pt(CO)_8(Ph_2P\text{-}Ⓟ)_2]$[7] [Ⓟ = poly(styrene–divinylbenzene)], exhibiting a carbonyl infrared spectrum similar to that of $[Fe_2Pt(CO)_8(PPh_3)_2]$ (Table I). The polymer-supported cluster $[RuPt_2(CO)_5(Ph_2P\text{-}Ⓟ)_3]$ was prepared by the reaction of $[RuPt_2(CO)_5(PPh_3)_3]$[8] with the functionalized polymer in toluene at 80 °C; the carbonyl infrared spectrum was similar to that of $[RuPt_2(CO)_5(PPh_3)_3]$[8] (Table I and Figure 1).

Two of the polymer-bound clusters, $[Fe_2Pt(CO)_8(Ph_2P\text{-}Ⓟ)_2]$ and $[RuPt_2(CO)_5(Ph_2P\text{-}Ⓟ)_3]$, were tested as ethylene hydrogenation catalysts in a flow system which allowed simultaneous measurement of the catalytic reaction rate and the infrared spectrum of the functioning catalyst.[9] With feeds of H_2, C_2H_4, and He at 98 °C and 1 atm, $[RuPt_2(CO)_5(Ph_2P\text{-}Ⓟ)_3]$ catalyzed ethylene hydrogenation at a typical rate of 10^{-2} molecules/Ru_2Pt cluster·s. The kinetics results obtained at 98 °C are well represented by

$$r = kKP_{H_2}{}^{1/2}P_{C_2H_4}/[(1 + KP_{C_2H_4})^2] \quad (1)$$

Table II. Kinetics of Ethylene Hydrogenation Catalyzed by $[RuPt_2(CO)_5(Ph_2P\text{-}Ⓟ)_3]$[a,b]

$$r = kKP_{H_2}{}^{1/2}P_{C_2H_4}/[(1 + KP_{C_2H_4})^2]$$

T, °C	$10^2 \times$ rate of ethylene hydrogenation,[c] molecules/$RuPt_2$ cluster·s	k,[d] molecules/$RuPt_2$ cluster·s·$atm^{1/2}$	K, atm^{-1}
73	8.2	0.48 ± 0.02	1.81 ± 0.14
87	14.3	0.85 ± 0.04	1.80 ± 0.21
98	19.8	1.04 ± 0.02	2.64 ± 0.18

[a] These parameters were estimated using a nonlinear least-squares regression technique. Best values of the parameters are given with 95% confidence limits. [b] Best values of the exponent on P_{H_2} were found to be 0.55 ± 0.06 at 73 °C, 0.58 ± 0.07 at 87 °C, and 0.49 ± 0.05 at 98 °C; a value of this exponent of 1/2 was used to represent the data at all three temperatures. [c] Rates measured at P_{H_2} = 0.73 and $P_{C_2H_4}$ = 0.20 atm. [d] The temperature dependence of k yields an activation energy of 7.8 ± 1.2 kcal/mol.

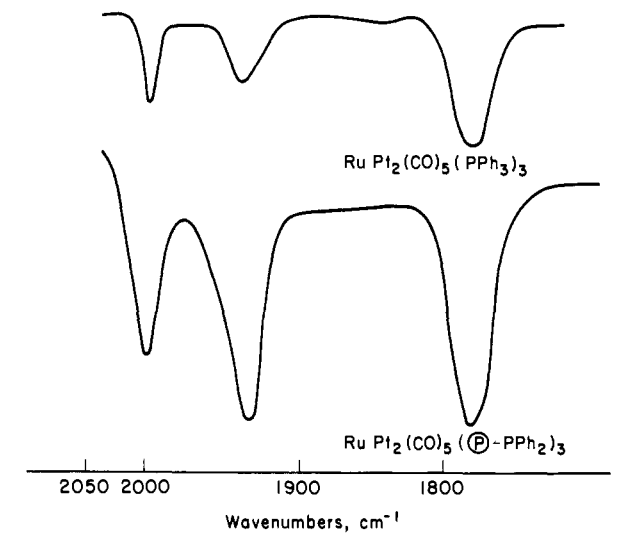

Figure 1. Comparison of the carbonyl infrared spectra of an 11-μm-thick membrane of $[RuPt_2(CO)_5(Ph_2P\text{-}Ⓟ)_3]$ and of $[RuPt_2(CO)_5(PPh_3)_3]$ in CH_2Cl_2 solution.

where r is reaction rate, P is partial pressure, k is a rate constant, and K is a temperature-dependent constant. The parameter values are summarized in Table II; the same equation fits the data obtained at other temperatures (Table II).

The kinetics suggests that the ethylene and hydrogen were both bonded to the metal catalyst. After 5 days on stream and ~4400 turnovers at 73 °C, the catalytic activity and the infrared spectrum remained unchanged, the spectrum indicating the presence of only one metal species, $[RuPt_2(CO)_5(Ph_2P\text{-}Ⓟ)_3]$. At 108 °C, however, there was a steady decrease in the intensities of the characteristic carbonyl absorptions with time on stream, and, after 1000 turnovers, the catalytic activity had increased about fourfold. The catalyst had changed from golden yellow to grayish brown, indicating that metal agglomeration had occurred.

$[Fe_2Pt(CO)_8(Ph_2P\text{-}Ⓟ)_2]$ catalyzed ethylene hydrogenation at 75 °C and 1 atm at a typical rate of 10^{-2} molecultes/$PtFe_2$ cluster·s. Preliminary kinetics data show that

$$r = kP_{H_2} \quad (2)$$

where k = 0.019 ± 0.002 molecules/Fe_2Pt cluster·s·atm. The data obtained at 85 and 95 °C indicated inhibition by substrate ethylene, being well represented by kinetics of the form of eq 1.

The similarity in the kinetics of ethylene hydrogenation

catalyzed by $[RuPt_2(CO)_5(Ph_2P\text{-}Ⓟ)_3]$ and $[Fe_2Pt(CO)_8(Ph_2P\text{-}Ⓟ)_2]$ is surprising; it suggests that the mechanisms were similar and that the clusters provided the active sites for hydrogenation. Different activities for the two catalysts would have been expected if the sites had been provided by aggregated metal.

The synthesis method was unsuccessful with some clusters. For example, contacting of $[H_2FeRu_3(CO)_{13}]$[10] with phosphine-functionalized silica at room temperature in hexane resulted in the formation of primarily $[Ru(CO)_4(Ph_2P\text{-SIL})]$ (SIL = silica) rather than a substituted metal cluster; attempts to prepare the silica-supported analogue of $[Fe_2Pt(CO)_8(PPh_3)_2]$ resulted in the decomposition of the cluster to give aggregated metal.

The silica-supported clusters $[H_2Os_3(CO)_9(Ph_2P\text{-SIL})]$[2] and $[HAuOs_3(CO)_{10}(Ph_2P\text{-SIL})]$[11] exhibited no measurable activity for propylene hydrogenation at 100 °C. These same two catalysts, however, were active for 1-butene isomerization at 110 °C, with $[H_2Os_3(CO)_9(Ph_2P\text{-SIL})]$ being ~10 times more active than $[HAuOs_3(CO)_{10}(Ph_2P\text{-SIL})]$.

Acknowledgment. This cooperative research was supported by NATO; the work in Delaware was supported by the National Science Foundation and the work in Munich by the Deutsche Forschungsgemeinschaft.

References and Notes

(1) J. H. Sinfelt and J. Cusumano, "Advanced Materials in Catalysis," J. J. Burton and R. L. Garten, Eds., Academic Press, New York, 1977, Chapter 1, pp 1–31.
(2) Similar attachment of triosmium (S. C. Brown and J. Evans, *J. Chem. Soc., Chem. Commun.*, 1063 (1978)) and tetrairidium (J. J. Rafalko, J. Lieto, B. C. Gates, and G. L. Schrader, Jr., *ibid.*, 540 (1978)) clusters has been reported, the latter having catalytic activity for olefin hydrogenation.
(3) C. Tamborski, F. E. Ford, W. L. Lehn, G. J. Moore, and E. J. Soloski, *J. Org. Chem.*, **27**, 619 (1962).
(4) H. Knözinger and E. Rumpf, *Inorg. Chim. Acta*, **30**, 51 (1978).
(5) Further characterization by ^{31}P NMR and laser Raman spectroscopy has so far been unsuccessful.
(6) M. I. Bruce, G. Shaw, and F. G. A. Stone, *J. Chem. Soc., Dalton Trans.*, 1082 (1972).
(7) More properly this formula should be represented as $[Fe_2Pt(CO)_8(Ph_2P\text{-}Ⓟ)_x(PPh_3)_{2-x}]$ (x = 1 or 2), but for simplicity throughout the text we write the formulas of the attached clusters assuming replacement of all PPh_3 groups by $Ph_2P\text{-}Ⓟ$ groups. Experiments to test the assumption are in progress.
(8) M. I. Bruce, G. Shaw, and F. G. A. Stone, *J. Chem. Soc., Dalton Trans.*, 1781 (1972).
(9) R. Thornton and B. C. Gates, *J. Catal.*, **34**, 275 (1974).
(10) G. L. Geoffroy and W. L. Gladfelter, *J. Am. Chem. Soc.*, **99**, 7565 (1977).
(11) L. J. Farrugia, J. A. K. Howard, P. Mitrprochochon, J. L., Spencer, F. G. A. Stone, and P. Woodward, *J. Chem. Soc., Chem. Commun.*, 260 (1978).

Ronald Pierantozzi, Kevin J. McQuade, Bruce C. Gates*
Center for Catalytic Science and Technology
Department of Chemical Engineering
University of Delaware, Newark, Delaware 19711
Margit Wolf, Helmut Knözinger, Werner Ruhmann
Institut für Physikalische Chemie der Universität München
8 München 2, West Germany
Received April 30, 1979

Structural Order in Liquid $CaCl_2 \cdot 6H_2O$

Sir:

Recently, increasing attention has been devoted to the microscopic structure and to possible structural changes that may take place with an increase of concentration in aqueous solutions of strong II–I electrolytes.[1,2] Indications obtained with different experimental techniques do not not always appear to be consistent, though great care should be used when comparing structural information from measurements of different observables.

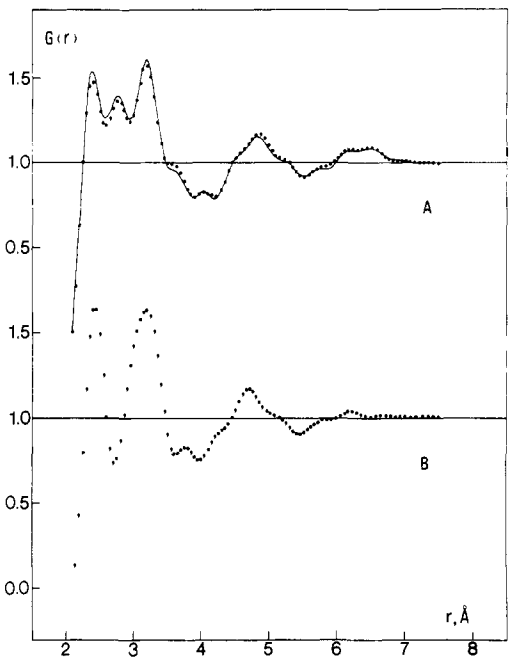

Figure 1. (A) Experimental (circles) and model (solid line) correlation functions for liquid $CaCl_2 \cdot 6H_2O$. (B) Experimental correlation function for the solution $CaCl_2 \cdot 12H_2O$.

Some open questions follow. Do qualitative changes in local order around ions occur and, if so, at what concentrations? Does the evolution of structural phenomena move toward an order more marked than the one involving only first hydration shells? Do very concentrated solutions show a tendency toward an order similar to the one existing in the corresponding hydrated crystal?

As diffraction patterns perhaps contain the most direct information about average molecular configurations in a liquid, meaningful contributions in clarifying these questions may come from X-ray diffraction studies on different electrolyte solutions, in a range of concentration including, when possible, the one with the same H_2O/salt ratio as the corresponding hydrated crystal.

Working within these general lines, we collected X-ray diffraction data from liquid $CaCl_2 \cdot 6H_2O$. As this hydrated salt melts near room temperature, it is possible to compare structural information obtained in this case with the results obtained under similar conditions in previous investigations on $CaCl_2$ aqueous solutions[3] with higher H_2O/salt ratios. From the diffracted intensities, measured in the range $0.3 < s < 15.5$ Å^{-1} ($s = 4\pi \sin\theta/\lambda$, θ being half the scattering angle and λ the wavelength of the Mo Kα radiation), we obtained the structure function, from which, via Fourier transform, the average correlation function $G(r)$ which describes the positional correlation between different atoms or ions in the system was calculated.

In the distance range containing information on nearest-neighbor interactions, the $G(r)$ curve for liquid $CaCl_2 \cdot 6H_2O$ (Figure 1A, circles) shows three resolved peaks centered at ~2.40, 2.75, and 3.20 Å, respectively; this curve is significantly different from the analogous one obtained[3] for the solution $CaCl_2 \cdot 12H_2O$ (Figure 1B) which exhibits a first peak at ~2.40 Å ascribed to sharp Ca^{2+}–H_2O interactions, a second peak at ~3.20 Å due to weaker Cl^-–H_2O interactions, and a deep minimum in the region 2.7 Å. It is therefore impossible to interpret the "structure" of the liquid $CaCl_2 \cdot 6H_2O$ as done in the case of less concentrated solutions, where X-ray diffraction data from solutions 1 to 4 M were explained[3] in terms of

0002-7863/79/1501-5438$01.00/0